INTERNATIONAL JOURNAL OF LATEST TECHNOLOGY IN ENGINEERING, MANAGEMENT & APPLIED SCIENCE (IJLTEMAS)

ISSN 2278-2540 | DOI: 10.51583/IJLTEMAS | Volume XIV, Issue X, October 2025

Study on Stability Evaluation of Concrete-Rockfill Combination Dam According to The Construction and Operation Stages

Yong Nam Ri*, Kuk Song Kim, Dok Yong Jong

Faculty of geological prospecting engineering, Kim Chaek University of Technology, 60 Kyogu, Yonggwang Street, Pyongyang 999093, Democratic People's Republic of Korea

DOI: https://doi.org/10.51583/IJLTEMAS.2025.1410000079

Received: 02 September 2025; Accepted: 10 September 2025; Published: 11 November 2025

Abstract- It is important to evaluate scientifically stability of dam and embankment in large-scale hydropower construction, tideland construction and preventing natural disasters. The aim of paper is to establish a method of stability assessment of concrete-rockfill combination dam (CRCD) as a new dam form. In this paper, we investigated the step loads acting during construction, operation and seismic operation and their corresponding stability assessment methods for CRCDs. According to the results, the slope stability is also an important indicator for the stability evaluation of CRCDs and the stability assessment method of rockfill dams may be applied to the stability assessment of CRCDs.

Keywords: Concrete-rockfill combination dam, Natural disaster, Slope stability, Stability evaluation.

I. Introduction

Dams and embankments are the most frequently used elements in the construction of hydraulic structures.

The shape and size of dam depend not only on the availability of building materials, but also on geological conditions, hydrological conditions and terrain conditions.

With the development of design and construction techniques, new dam forms are also emerging. Concrete-rockfill combination dam (CRCD) is an intermediate type of concrete gravity dam (CGD) and rockfill embankment, which makes it possible to obtain many reserves in dam construction.

Currently, concrete and rockfill materials are commonly used in dam construction. There are many kinds of concrete dams, of which gravity dams provide the stability of the dam by maintaining the hydraulic pressure, earth pressure, uplift pressure, etc. by their own weight. Therefore, the stability of CGDs is usually directly proportional to the amount of concrete being constructed. Also, temperature control and crack development are major problems in CGDs (Arici 2013; Bazant 1996; Bouzoubaâ et al. 1997; Campos et al. 2016).

The rockfill dams can be divided into the sloping upstream core dam (SUCD) and the central core dam (CCD) according to the location of impervious core, which uses low permeability materials such as clay, pitch, concrete, etc. In rockfill dam construction, there is a high demand for impervious core materials, which clay is commonly used, and concrete is used if there is no clay near the construction site. Concrete-faced rockfill dams using concrete as impervious material are known to be convenient in construction as well as good seismic performance, but non-uniform settlement can cause cracks in concrete slabs and cause instability in the dam (Ri et al. 2022; Xu, Zou, and Liu 2012). In addition, rockfill dams are generally characterized by a large amount of filling volume.

In order to overcome the limitations of traditional CGDs and concrete-faced rockfill dams, a new CRCD can be used. CRCD is mainly composed of upstream concrete walls and downstream inclined rockfill bodies to support hydraulic pressure. Among these, concrete wall is impervious structure of CRCD, which not only reduce the amount of concrete compared to CGD, but also improve strength and impermeability compared to concrete panels of concrete-faced rockfill dam. In addition, the inclined rockfill mass downstream has the advantage of saving rockfill material compared to conventional rockfill dams.

Many previous researchers have carried out numerical simulations of rockfill dams and analyzed the deformation, settlement, acceleration distribution behaviour and seismic reliability of the dam body after earthquake, and only some researchers have considered the influence of pore water pressure and permeability of the dam material on seismic behaviour.

Pang et al. (Pang et al. 2018) proposed a new methodology combining generalized probability density evolution method (GPDEM) with spectral representation-random function method to evaluate seismic reliability, and concluded that the simulation results considering non-softening and softening behaviour s of rockfill materials are more and more different when seismic intensity is high, and it is more reasonable to use time accumulation of safety factor rather than safety factor in estimating seismic reliability of dam slopes.

Li et al. (Li, Wang, and Du 2020) extended the procedure of probabilistic seismic slope displacement hazard analysis (PSSDHA) by combining the spatial variability of the soil strength parameters c′ and φ′ and systematically investigated the influence of spatial variability on slope displacement hazard. The results clearly showed that neglecting the spatial variability of soil parameters can

ISSN 2278-2540 | DOI: 10.51583/IJLTEMAS | Volume XIV, Issue X, October 2025

underestimate the displacement hazard, and such underestimation is more important as the scale of vibration decreases (i.e., soils with high heterogeneity) or c′□tanφ′ correlation decreases.

Some researchers have conducted a reduced model experiment and numerical simulation of a concrete gravity dam and studied the crack generation, failure and other dynamic behaviour due to the seismic response. And some studies have also carried out numerical simulations of concrete retaining walls and shaking table model tests, and investigated the failure mechanism of retaining walls during earthquakes, the influence of various factors on seismic behaviour, and dynamic earth pressure behaviour during earthquakes.

Mridha et al. (Mridha and Maity 2014) investigated experimentally the nonlinear response of the concrete gravity dam-reservoir system on a horizontal shaking table using sinusoidal wave modulation motion for the small-scale model of Koyna dam. The experiments were conducted in a dam-reservoir system with empty reservoir and full reservoir by applying horizontal sinusoidal wave linear frequency modulation excitation to the shaking table to observe the foundation behaviour, crack formation, crack opening, slip along the crack plane, and stability after crack formation in the dam model. Numerical analysis of the system was also carried out in ABAQUS 6.14-4 using the fracture-plastic model.

Zhu et al. (Zhu et al. 2021) studied the failure mechanism of geocell flexible reinforced retaining walls under earthquake using FLAC3D nonlinear finite difference method, analyzed the advantage of the geocell flexible reinforced retaining walls by comparing the geogrid reinforced retaining wall with the non-reinforced retaining wall, and investigated the deformation of the reinforced wall by varying the length of the geocell and the reinforcement spacing. The results showed that the geocell can effectively reduce the horizontal displacement of the retaining wall and its effect is better than the geogrid.

Hosseinzadeh et al. (Hosseinzadeh, Soroush, and Shafipour 2022) conducted finite element dynamic analysis for qualitative and quantitative assessment of dynamic earth pressure in buildings with basement and considered different excavation depths, ground topography, geotechnical parameters, and above-ground building layers in the analysis. Using the obtained results, soil-structure interaction responses were discussed and approximate relationships were derived to evaluate dynamic earth pressure.

Recently, some researchers have published the seismic behaviour and seismic reliability of CRCDs by means of shaking table tests and numerical simulations.

Le´ger et al. (Le´ger and Javanmardi 2007) considered a typical 35m high concrete gravity dam strengthened by rockfill buttressing and confirmed that rockfill can improve the seismic stability of a gravity dam by applying pressure to a concrete dam against hydrostatic loads, and found that by means of numerical analysis, notable passive (or active) earth pressure cannot develop in composite dams with a finite backfill width.

Wang et al. (Wang et al. 2017) used a large-scale shaking table test to reproduce the seismic response of a CRCD and carried out a series of measurements of the acceleration, dynamic earth pressure, deformation and slope failure mode of the dam according to PGA. The results showed that the CRCD model shows good seismic performance with small residual deformation under earthquake.

Wang et al. (Wang, Yang, and Tang 2022) conducted small-scale CRCD model tests using a large shaking table and analyzed the displacement, stability and dynamic earth pressure of the CRCD to provide basic data for earthquake-proof design.

Up to date, there is no extensive research on CRCDs and it has not been actively applied in construction practice. However, CRCDs are an economical dam type and it is important to solve the problems in its design calculations. In particular, it is important to consider the stability of CRCD in viewpoint of step loads acting in the construction and operation stages. But, in previous studies, the stability behaviour of CRCDs is not clearly understood in viewpoint of step loads and there are many cases where the purely mechanical aspect is biased.

In this paper, the stability behaviour of CRCDs is investigated in relation to the step loads by transient analysis using the seepage-stress coupled finite element method.

Stability Assessment Method of CRCD

Mechanical material models

The Mohr-Coulomb model shows good applicability in many practical problems of geotechnical engineering. Because its material parameters are easy to obtain, it is widely used in numerical simulations of geotechnical engineering. The Mohr-Coulomb model is used for both the ground and the rockfill. The parameters required for this model are determined by geotechnical tests.

The Mohr-Coulomb model is written by three stress invariants in the general stress state as (Menétrey and Willam 1995):

$$F = R_{mc} q - p \tan\phi - c = 0 \tag{1}$$

where $R_{mc}(\theta,\phi) = \frac{1}{\sqrt{3}\cos\phi}\sin\left(\theta+\frac{\pi}{3}\right)+\frac{1}{3}\cos\left(\theta+\frac{\pi}{3}\right)\tan\phi$. ϕ is the slope of the Mohr-Coulomb yield surface in $p - R_{mc}q$ stress plane. This is generally referred to as the material friction angle and can depend on the temperature and predefined

ISSN 2278-2540 | DOI: 10.51583/IJLTEMAS | Volume XIV, Issue X, October 2025

field variables in ABAQUS program. *c* is the cohesion of material and θ is the deviatoric polar angle defined as $\cos(3\theta)=\left(\frac{r}{q}\right)^3$.

And $p=-\frac{1}{3}trace(\boldsymbol{\sigma})$ is the equivalent pressure stress. $q=\sqrt{\frac{3}{2}(\mathbf{S}:\mathbf{S})}$ is the Mises equivalent stress, $r=\left(\frac{9}{2}\mathbf{S}\cdot\mathbf{S}:\mathbf{S}\right)^{\frac{1}{3}}$ is the third invariant of deviatoric stress, $\mathbf{S}=\boldsymbol{\sigma}+p\mathbf{I}$ is the stress deviator. The friction angle, ϕ controls the shape of the yield surface in the deviatoric plane. The friction angle can be in the range of $0°\le\phi\le 90°$. In the case of $\phi=0°$ the Mohr-Coulomb model reduces to the pressure-independent Tresca model with a perfectly hexagonal deviatoric section. In the case of $\phi=90°$ the Mohr-Coulomb model would reduce to the "tension cut-off" Rankine model with a triangular deviatoric section and $R_{mc}=\infty$.

A concrete damaged plasticity model is used for the concrete wall.

In the concrete damaged plasticity model, it is assumed that the uniaxial tensile and compressive response of concrete is characterized by the damaged plasticity, as shown in Fig. 1 (Hillerborg, Modeer, and Petersson 1976; Lubliner et al. 1989; Wang et al. 2019).

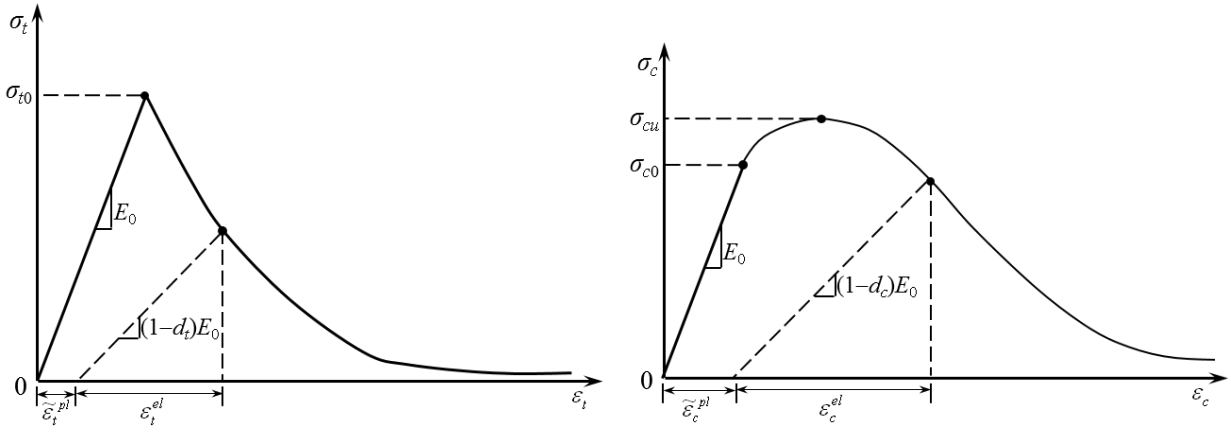

(a) Tensile (b) Compression

Fig 1: Concrete response to uniaxial loading conditions.

The stress-strain response under uniaxial tension follows a linear elastic relationship until the failure stress σ_{t0} is reached. The failure stress corresponds to the development of microcracks in concrete material. In addition to the failure stress, the formation of microcracks is macroscopically represented by the softening stress-strain response, which induces strain localization in the concrete structure. Under uniaxial compression, the response is linear to the initial yield stress value σ_{c0}. Under plastic conditions, the response is typically characterized by stress hardening and is strain-softened beyond the ultimate stress σ_{cu}. This is somewhat simplified, but represents the basic feature of the response of the concrete.

As shown in Fig. 1, when a concrete specimen is unloaded at any point on the strain-softening branch of the stress-strain curve, the unloading response is weakened, i.e. the elastic stiffness of the material is damaged (or degraded). The degradation of the elastic stiffness is characterized by two damage variables, d_t and d_c, which in the ABAQUS program are assumed to be a function of the plastic strain, temperature, and field variables.

$$d_t=d_t\left(\tilde{\varepsilon}_t^{pl},\theta,f_i\right);\ 0\le d_t\le 1$$
$$d_c=d_c\left(\tilde{\varepsilon}_c^{pl},\theta,f_i\right);\ 0\le d_c\le 1 \quad (2)$$

Here, the subscripts *t* and *c* represent the tensile and compressive, respectively. $\tilde{\varepsilon}_t^{pl}$ and $\tilde{\varepsilon}_c^{pl}$ are the equivalent plastic strains, θ is the temperature in the ABAQUS program, and f_i, (i=1, 2,...) is a predefined field variable.

Damage variables can take values from zero representing the undamaged material to a value representing the strength total loss.

ISSN 2278-2540 | DOI: 10.51583/IJLTEMAS | Volume XIV, Issue X, October 2025

If E_0 is the initial (undamaged) elastic stiffness of the material, the stress-strain relationship under uniaxial tension and compression loading is respectively

$$\sigma_t = (1-d_t)E_0\left(\varepsilon_t - \tilde{\varepsilon}_t^{pl}\right)$$
$$\sigma_c = (1-d_c)E_0\left(\varepsilon_c - \tilde{\varepsilon}_c^{pl}\right) \quad (3)$$

The "effective" tensile and compressive cohesive stresses that determine the size of the yield (or failure) surface are defined as follows:

$$\bar{\sigma}_t = \frac{\sigma_t}{(1-d_t)} = E_0\left(\varepsilon_t - \tilde{\varepsilon}_t^{pl}\right)$$
$$\bar{\sigma}_c = \frac{\sigma_c}{(1-d_c)} = E_0\left(\varepsilon_c - \tilde{\varepsilon}_c^{pl}\right) \quad (4)$$

Permeability model

The constitutive equation for pore fluid flow in unsaturated soils is usually given by Darcy's law or Forchheimer's law. According to Forchheimer's law, the negative gradient of the pressure head is related to a quadratic function of the volume flow rate of the wetting liquid through a unit area of medium (Desai 1975).

$$sn\mathbf{v}_w\left(1+\beta\sqrt{\mathbf{v}_w\cdot\mathbf{v}_w}\right) = -\hat{\mathbf{k}}\cdot\frac{\partial\Phi}{\partial\mathbf{x}} \quad (5)$$

Where $\hat{\mathbf{k}}$ is the permeability of the medium and Φ is the pressure head defined as.

$$\Phi = z + \frac{u_w}{g\rho_w} \quad (6)$$

Where *z* is the elevation above a reference surface and *g* is the acceleration of gravity acting in the opposite direction to *z*. $\mathbf{v}_w$ is the velocity of the fluid and β is the velocity coefficient (Tariq 1987). If $\beta = 0$, Forchheimer's law is equal to Darcy's law.

We assume that the permeability of unsaturated soil depends on the degree of saturation as follows.

$$\hat{\mathbf{k}} = k_s\mathbf{k} \quad (7)$$

Here, $\mathbf{k}$ is the permeability for a fully saturated soil.

During the seepage-stress coupling analysis, the change of the stress field causes the change of the void ratio, and the change of the void ratio changes the saturated permeability of the soil mass. The change of the saturated permeability with the change of the void ratio is determined by experiments and, in the absence of experimental results, empirical equations can be used.

And k_s is the relative permeability dependent on the degree of saturation, where $k_s(1) = 1.0$. Nguyen et al. (Nguyen and Durso 1983) found that the permeability in steady flow through a partially saturated medium varies with s^3.

s is the degree of saturation. If s is equal to the effective degree of saturation, according to Van Genuchten (Van Genuchten 1980), it is expressed by the unsaturated parameters *α*, *n* as.

$$s = \left[1+\left(\frac{\alpha u_w}{\gamma_w}\right)^n\right]^{-m} \quad (8)$$

Here, $m = 1-\frac{1}{n}$ and γ_w is the volume weight of wetting fluid.

Loads and stability analysis

The CRCD generally has the structure as Fig. 2. As can be seen in the figure, this type of dam may be seen as it which removes the upstream rockfill in concrete central core rockfill dams (Wang et al. 2017; Wang, Yang, and Tang 2022). Alternatively, it can be

ISSN 2278-2540 | DOI: 10.51583/IJLTEMAS | Volume XIV, Issue X, October 2025

seen that the CGD has a reduced cross-section and an additional rockfill on the downstream side corresponding to a reduced concrete volume. Otherwise, we may consider this structure as a retaining wall subjected to hydraulic loading from the concrete wall side.

Therefore, the stability assessment methods of rockfill dam, CGD and retaining wall should be properly combined in the stability assessment of CRCDs.

The stability of CRCDs should also be examined for the most unfavorable load combination conditions during construction and operation as well as the stability evaluation of other dams.

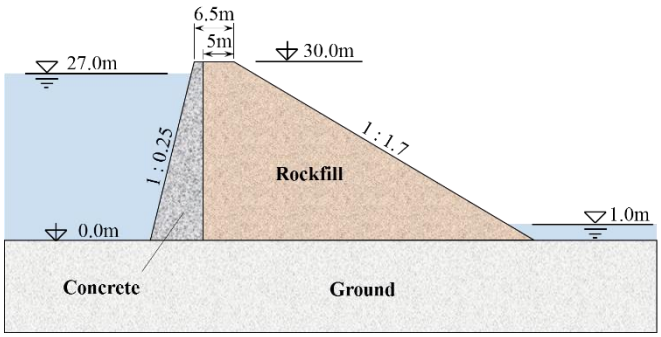

Fig 2: Cross section of CRCD

Table 1 shows the stability evaluation index and the load to be considered for CRCDs. As shown in the table, the stability of sliding, overturning, bearing capacity, and slope activity in CRCDs should be evaluated. And the calculation of safety factor should consider mainly the concrete and rockfill mass, hydraulic pressure and earth pressure. Seismic load should be considered in the earthquake case, along with the concrete and rockfill mass, hydraulic pressure and earth pressure. In the case of relatively large bottom width of concrete wall, the uplift pressure also has a significant effect on the stability of CRCD. The wave pressure, sedimentary earth pressure and ice pressure are not large but affect the stress and stability of CRCD. Calculation method of earth pressure shall be changed during construction or operation periods.

Table 1: Stability Evaluation indices and Load Combinations for CRCD

		Stability Indices			
		Sliding	Overturning	Bearing Capacity	Slope Activity
Construction Period	Assessment	○	○	○	×
	Loads Considered	Concrete self-weight, Active earth pressure	Concrete self-weight, Active earth pressure	Concrete self-weight	
Operation Period	Assessment	○	○	×	○
	Loads Considered	Hydraulic pressure, Concrete self-weight, Passive earth pressure, Uplift pressure	Hydraulic pressure, Concrete self-weight, Passive earth pressure, Uplift pressure		Hydraulic pressure, Groundwater flow, Rockfill self-weight
Earthquake Period	Assessment	○	○	×	○
	Loads Considered	Hydraulic pressure, Concrete self-weight, Earth pressure, Uplift pressure, Ground vibration	Hydraulic pressure, Concrete self-weight, Earth pressure, Uplift pressure, Ground vibration		Hydraulic pressure, Groundwater flow, Rockfill self-weight, Ground vibration

Stability Evaluation: Case Study

The cross-section of CRCD is shown in Fig. 2, and the physical and mechanical properties of the material are shown in Table 2. The friction coefficient between ground and concrete is f=1.1 and the adhesion force between ground and concrete is not considered in the stability evaluation.

In this case study, the stability of the earthquake period is not addressed. During the earthquake, the step loads such as earth pressure, hydraulic pressure, seismic inertia, etc. change with time, and thus the safety factors change dynamically for sliding, overturning,

ISSN 2278-2540 | DOI: 10.51583/IJLTEMAS | Volume XIV, Issue X, October 2025

bearing capacity, and slope activity. The stability change characteristics will depend on the time-dependent nature of the seismic acceleration and the seismic intensity. The stability assessment of CRCD during earthquake requires more detailed investigation compared to the stability assessment of construction and operation periods. Therefore, the study of the stability change characteristics during earthquake will remain a subject of future research.

Fig. 3 shows the phreatic surface developed in the CRCD during operation period, while the level of phreatic surface in the rockfill is relatively high. The unit flow rate of reservoir water through dam and ground is about 77.8 $m^3/d(m)$.

Fig. 4 shows the displacement vector of CRCD during construction and operation periods, respectively. According to the displacement vector, its maximum value is 41.25 mm at construction period and 42.27 mm at operation period, respectively, in the rockfill near the dam crest. Also, during operation, the horizontal component of displacement is more strongly represented, especially the downward component of displacement is clearly seen in the concrete wall near the crest and in the rockfill below the phreatic surface.

Fig. 5 and Fig. 6 show the vertical stress distribution and shear stress distribution in the CRCD and ground during construction and operation periods, respectively.

According to the vertical stress distribution, no tensile stress exists at the bottom of the concrete wall during construction, and during operation, tensile stress develops in the upstream heel of the concrete wall and compressive stress in the downstream toe. In other words, no tensile stress-induced failure is expected in the concrete wall during construction, and the effect of rotation is obvious in the concrete wall during operation, which is caused by the hydraulic pressure. The magnitude of tensile stress developed in the upstream heel during operation is around 0.89MPa, which satisfies the tensile stress limit of concrete.

According to the shear stress distribution, it is found that the shear stress is concentrated in the upstream heel and downstream toe of the concrete wall at the operation period than at the construction period due to the effect of the hydraulic pressure acting on the concrete wall. Therefore, it is important to take reinforcement measures for the upstream heel and downstream toe of the concrete wall.

Fig. 7 shows the potential sliding failure (potential slope active) zones in rockfill during construction and operation. According to the figures, the shape of the plastic failure zones is almost similar in both cases. However, in more detail, there is little difference in the vicinity of the toes of the rockfill, with the plastic failure zone developing deeper in the operation period compared to the construction period. In other words, during construction, the plastic failure (slope active) zone starts at the toe of the rockfill and develops upstream with a certain angle, but during operation, the plastic failure (slope active) zone starts at the toe of the rockfill and develops almost horizontally upstream, due to the influence of seepage flow. This leads to a difference in the safety factor of slope activity.

Table 3 shows the results of safety factors according to the load combinations of Table 1. Since the CRCD is placed on the rock mass, the safety factor for the bearing capacity has not been examined. In addition, the safety factors for earthquakes are not considered here because they are the subject of further research.

The results of Table 3 show that all safety factors have sufficient margin during construction and operation periods.

As shown in the table, during the construction period, the safety factor of sliding is the largest, 4.33, and the safety factor of slope activity is the smallest, 2.02. And during operation, the safety factor of overturning is the largest, with 3.99, and the safety factor of slope activity is the smallest, with 1.76. This suggests that the activity stability of slope in rockfill is an important indicator for the stability assessment of CRCD. In other words, it is shown that the stability assessment method of rockfill dams can be applied when assessing the stability in CRCD, except in the special case where the bond between the ground and the concrete wall is broken.

Table 2: Physical and Mechanical Properties of Materials

Material	E(GPa)	v	ρ(kg/m^3)	c(kPa)	φ(°)	k(m/d)
Concrete	24.0	0.20	2400	-	-	0.00864
Ground	30.0	0.25	2400	-	-	4.32
Rockfill	0.1	0.33	1840	20	40	25.92

ISSN 2278-2540 | DOI: 10.51583/IJLTEMAS | Volume XIV, Issue X, October 2025

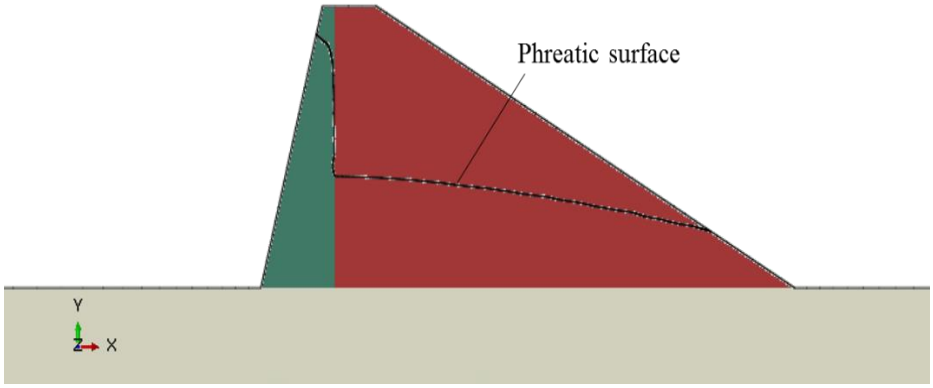

Fig 3: Phreatic surface (Operation period)

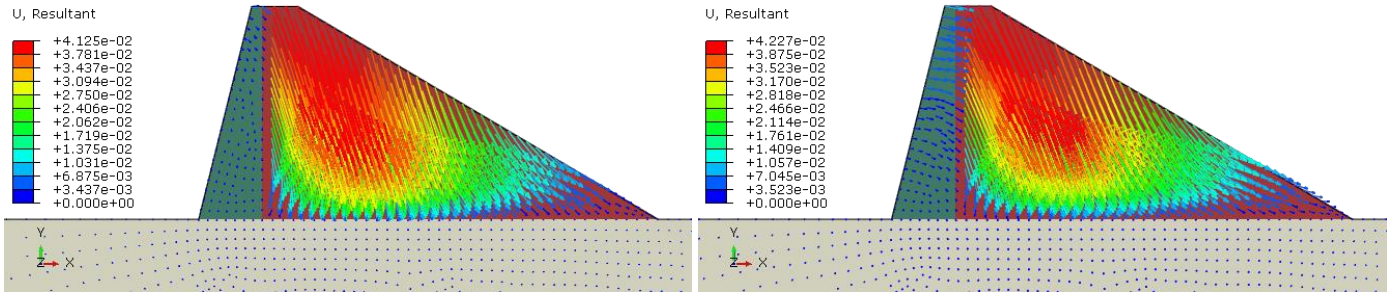

(a) Construction period (b) Operation period

Fig 4: Displacement vector

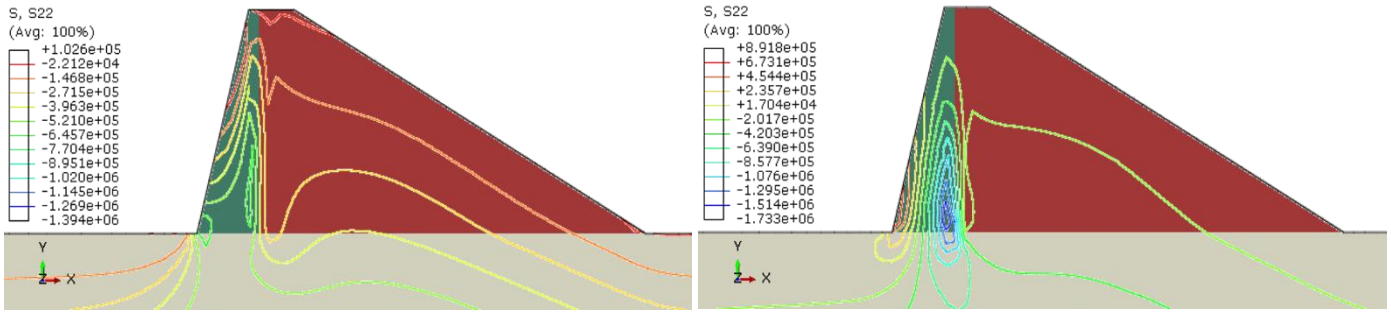

(a) Construction period (b) Operation period

Fig 5: Vertical stress

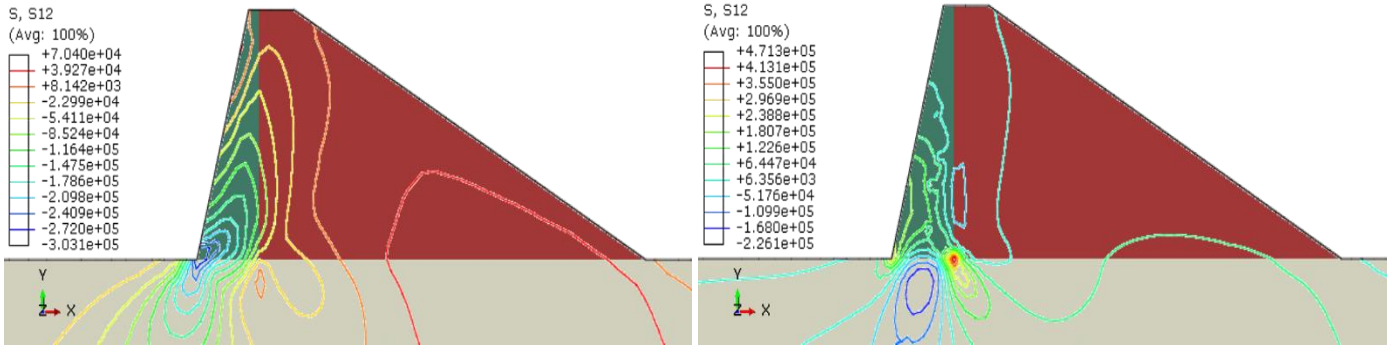

(a) Construction period (b) Operation period

Fig 6: Shear stress

ISSN 2278-2540 | DOI: 10.51583/IJLTEMAS | Volume XIV, Issue X, October 2025

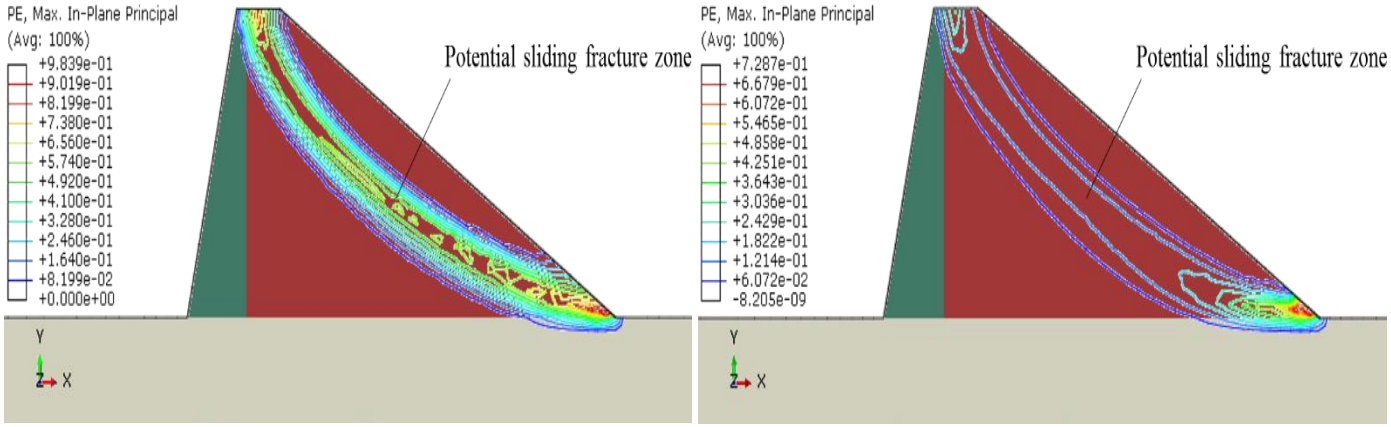

(a) Construction period (b) Operation period

Fig 7: Potential plastic failure zones in rockfill

Table 3: Safety Factors Calculated

	Safety Factor		
	Sliding	Overturning	Slope Activity
Construction Period	4.33	2.37	2.02
Operation Period	3.86	3.99	1.76

II. Conclusion

This paper have described the concept of CRCD, the advantages, the stability assessment method of CRCD and the case study.

According to the above results, the following conclusions can be drawn:

First, the safety factor of slope activity is generally the lowest compared to the safety factors of sliding or overturning during construction and operation, which means that the slope activity stability of rockfill is an important parameter in the stability evaluation of CRCDs. Therefore, the stability assessment method of rockfill dams may be applied to the stability assessment of CRCDs.

Second, according to the stress results in the concrete wall, it should be noted that during operation, tensile stress is generated on the upstream side of the concrete wall and crack occurs.

Third, the rockfill material should be a highly permeable material that generates sufficient earth pressure.

CRCD is dam type that allow economic benefits when compared to CGDs or concrete core dams, which can be widely applied in the constructions of reservoir or tide embankment.

Further studies are needed to investigate the stability change characteristics of CRCD during earthquake.

III. Acknowledgment

The research reported in this paper is sponsored by the Academy of Science of the D.P.R. Korea and the Design Research Institute of Electrical Power of Pyongyang. The technical support given by these sponsors is greatly appreciated. The authors are grateful to acknowledge for many helps and advices of all persons for this research project, and also thank for the trouble editors and reviewers have taken.

References

1. Arici, Y. 2013. Evaluation of the performance of the face slab of a concrete face rockfill dam during earthquake excitation. Soil Dynamics and Earthquake Engineering 55 (6): 71–82.
2. Bazant, Z. P. 1996. Is no-tension design of concrete or rock structures always safe?-fracture analysis. Journal of Structural Engineering 122 (1): 2–10.
3. Bouzoubaâ, N., M. Lachemi, B. Miao, and P. C. Aïtcin. 1997. Thermal damage of mass concrete: Experimental and numerical studies on the effect of external temperature variations. Canadian Journal of Civil Engineering 24 (4): 649–57.
4. Campos, A., C. López, A. Blanco, and A. Aguado. 2016. Structural diagnosis of a concrete dam with cracking and highnonrecoverable displacements. Journal of Performance of Constructed Facilities 30 (5): 1–12.
5. Desai, C. S. 1975. Finite element methods for flow in porous media. In Finite Elements in Fluids 1: 157–81.

ISSN 2278-2540 | DOI: 10.51583/IJLTEMAS | Volume XIV, Issue X, October 2025

6. Hillerborg, A., M. Modeer, and P. E. Petersson. 1976. Analysis of Crack Formation and Crack Growth in Concrete by Means of Fracture Mechanics and Finite Elements. Cement and Concrete Research 6: 773–82.
7. Hosseinzadeh, A., A. Soroush, and R. Shafipour. 2022. A comprehensive numerical analysis of EQ-induced lateral earth pressure on structures basement walls. Soil Dynamics and Earthquake Engineering 163: 107521.
8. Le´ger, P., and F. Javanmardi. 2007. Seismic stability of concrete gravity dams strengthened by rockfill buttressing. Soil Dynamics and Earthquake Engineering 27: 274–290.
9. Li, D. Q., M. X. Wang, and W. Q. Du. 2020. Influence of spatial variability of soil strength parameters on probabilistic seismic slope displacement hazard analysis. Engineering Geology 1-41.
10. Lubliner, J., J. Oliver, S. Oller, and E. Oñate. 1989. A Plastic-Damage Model for Concrete. International Journal of Solids and Structures 25: 299–329.
11. Menétrey, Ph., and K. J. Willam. 1995. Triaxial Failure Criterion for Concrete and its Generalization. ACI Structural Journal 92: 311-18.
12. Mridha, S., and D. Maity. 2014. Experimental investigation on nonlinear dynamic response of concrete gravity dam-reservoir system. Engineering Structures 80: 289–97.
13. Nguyen, H. V., and D. F. Durso. 1983. Absorption of water by fiber webs: an illustration of diffusion transport. In Tappi Journal 66 (12).
14. Pang, R., B. Xu, X. J. Kong, D. G. Zou, and Y. Zhou. 2018. Seismic reliability assessment of earth-rockfill dam slopes considering strain-softening of rockfill based on generalized probability density evolution method. Soil Dynamics and Earthquake Engineering 107: 96–107.
15. Ri, Y. N., U. Ch. Han, U. J. Jang, D. Y. Jong, and Ch. U. Kim. 2022. Study on Stability Reduction Characteristics of Earth and Rockfill Dams under Rapid Drawdown Using Fully Coupled Seepage-Stress Analysis. Advances in Civil Engineering 2022: 1-13.
16. Tariq, S. M. 1987. Evaluation of flow characteristics of perforations including nonlinear effects with the finite element method. In SPE Production Engineering 1987: 104–12.
17. Van Genuchten, M. T. 1980. A closed-form equation for predicting the hydraulic conductivity of unsaturated soils. Soil Science Society of America Journal 44: 892–98.
18. Wang, H. T., J. Y. Shen, F. Wu, Zh. Q. An, and T. Y. Liu. 2019. Experimental study on elastic-plastic seismic response analysis of concrete gravity dam with strain rate effect. Soil Dynamics and Earthquake Engineering 116 (2019): 563–69.
19. Wang, J. X., G. Yang, H. L. Liu, S. S. Nimbalkar, X. J. Tang, and Y. Xiao. 2017. Seismic response of concrete-rockfill combination dam using large-scale shaking table tests. Soil Dynamics and Earthquake Engineering 99 (2017): 9–19.
20. Wang, J. X., G. Yang, and X. J. Tang. 2022. Test on Stability of Concrete-Rockfill Combination Dam. JOURNAL OF EARTHQUAKE ENGINEERING 26 (16): 8706–23.
21. Xu, B., D. G. Zou, and H. B. Liu. 2012. Three-dimensional simulation of the construction process of the Zipingpu concrete face rockfill dam based on a generalized plasticity model. Computers and Geotechnics 43 (6): 143–54.
22. Zhu, Y. L., K. Tan, Y. Hong, T. Tan, M. R. Song, and Y. X. Wang. 2021. Deformation of the Geocell Flexible Reinforced Retaining Wall under Earthquake. Advances in Civil Engineering 1–11. Article ID 8897009.